

where $E_N^{(n)}$ is the related error for which the estimation

$$E_N^{(n)} \leq \frac{\rho_e^{2N}}{2^{3N-1} N! \sqrt{(\pi_e)}} \sum_{k=1}^n \eta_k^{2N}$$

corresponds. Using

$$\frac{2}{\sqrt{(\pi)}} \int_0^x e^{-u^2} du = \frac{2}{\sqrt{(\pi)}} \sum_{l=0}^{+\infty} \frac{(-1)^l}{l! (2l+1)} x^{2l+1}$$

and averaging eqn. 10 with respect to the phase φ , the final relation for bit error rate is obtained¹

$$P_e = \frac{1}{2} - \frac{1}{\sqrt{(\pi)N^n}} \sum_{k_1=1}^N \dots \sum_{k_n=1}^N \sum_{l=0}^{+\infty} \frac{(-1)^l \left(\frac{\rho_e}{\sqrt{(2)}}\right)^{2l+1}}{l! (2l+1)} \times \{B(\rho_s, \rho_e, \eta_i) + C(\rho_s, \rho_e, \eta_i)\} + E_N^{(n)} \quad (11)$$

where

$$B(\rho_s, \rho_e, \eta_i) = \sum_{l_1=0}^{(2l_1+1)/2} \binom{2l_1+1}{2l_1} D_i^{2l_1+1-2l_1} \frac{1}{4^{l_1}} \times \left\{ \binom{2l_1}{l_1} + \sum_{j=0}^{l_1-1} 2 \binom{2l_1}{j} \left(\frac{\rho_s}{\sqrt{(2)}}\right)^{2l_1-2j} \right\} \times \frac{\Gamma(l_1-j+1)}{(2l_1-2j)!} {}_1F_1(l_1-j, 2l_1-2j+1, -\rho_s^2/2)$$

$$C(\rho_s, \rho_e, \eta_i) = \sum_{l_2=1}^{(2l_2+1)/2+1} \binom{2l_2+1}{2l_2-1} D_i^{2l_2-2l_2+2} \frac{1}{2^{2l_2-2}} \times \sum_{j=0}^{l_2-1} \binom{2l_2-1}{j} \left(\frac{\rho_s}{\sqrt{(2)}}\right)^{2l_2-2j-1} \times \frac{\Gamma(l_2-j+0.5)}{(2l_2-2j-1)!} \times {}_1F_1(l_2-j-0.5, 2l_2-2j, -\frac{\rho_s^2}{2})$$

$$D_i = \sum_{i=1}^n \eta_i \cos(2k_i - 1) \frac{\pi}{2N}$$

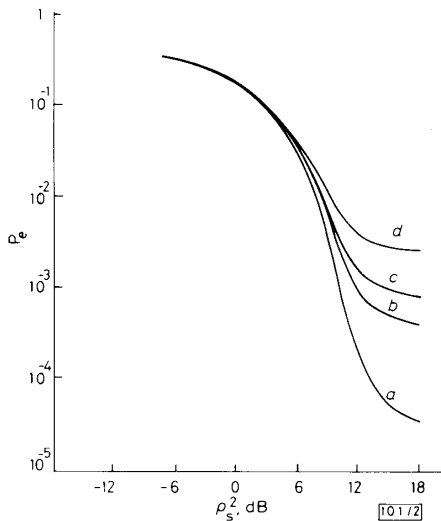


Fig. 2 Bit error rate of digital phase modulated signal plotted against SNR at the satellite input (ρ_s^2) for various values of SNR at the earth station input (ρ_e^2)

- a $\rho_e^2 = 12$ dB $\left. \begin{matrix} \eta_1^2 = \eta_2^2 = \eta_3^2 = -\infty$ dB
- c $\rho_e^2 = 10$ dB
- b $\rho_e^2 = 12$ dB $\left. \begin{matrix} \eta_1^2 = -20$ dB $\eta_2^2 = -14$ dB $\eta_3^2 = -20$ dB
- d $\rho_e^2 = 10$ dB

where ${}_1F_1(\cdot)$ is the confluent hypergeometric series and $\Gamma(\cdot)$ is the gamma function and $[\cdot]$ means integer part of the value inside.

In Fig. 2 the bit error rate of digital phase modulated signals transmitted over the satellite channel is plotted against SNR at the satellite input (ρ_s^2) for various values of SNR at the earth station input (ρ_e^2). The interference in this case is approximated by three sinusoidal signals. The existence of interference increases bit error rate, and this influence increases with increasing SNR at the earth station input.

M. Č. STEFANOVIĆ
Z. B. NIKOLIĆ

29th February 1988

Faculty of Electronic Engineering
University of Niš
Beogradska 14, 18000 Niš
Yugoslavia

References

- 1 JAIN, P., and BLACHMAN, N.: 'Detection of a PSK signal transmitted through a hard-limited channel', *IEEE Trans.*, 1973, **IT-19**, p. 623
- 2 KOSTIĆ, I.: 'Error rates of DCPK signals in hard limited multilink systems with co-channel interference and noise', *IEEE Trans.*, 1982, **COM-30**, pp. 222-230
- 3 STEFANOVIĆ, M.: 'Performance of signals coded by Miller code in the presence of noise and interference', *Electron. Lett.*, 1985, **21**, pp. 667-668
- 4 SCHWARTZ, M.: 'Information transmission, modulation and noise' (McGraw-Hill, New York, 1959)

GaAs/AlGaAs HETEROJUNCTION Pnp BIPOLAR TRANSISTORS GROWN ON (100) Si BY MOLECULAR BEAM EPITAXY

Indexing terms: Semiconductor devices and materials, Bipolar devices, Transistors, Silicon

GaAs/AlGaAs Pnp heterojunction bipolar transistors (HBTs) were fabricated and tested on (100) Si substrates for the first time. A common-emitter current gain of $\beta = 8$ was measured for the typical devices with an emitter area of $50 \times 50 \mu\text{m}^2$ at a collector current density of 1×10^4 A/cm² with no output negative differential resistance up to 280 mA, highest current used. A very high base-collector breakdown voltage of 10 V was obtained. Comparing the similar structures grown on GaAs substrates, the measured characteristics clearly demonstrate that device grade hole injection can be obtained in GaAs on Si epitaxial layers despite the presence of dislocations.

Recently, epitaxial growth of GaAs on Si has been attracting a great deal of attention because of the promise of combining both III-V and more technologically mature silicon devices on a Si substrate. The extent of success already obtained makes the growth of GaAs devices on Si well worth investigating. GaAs/AlGaAs Npn heterojunction bipolar transistors (HBTs) on Si with current gain frequencies of $f_t = 30$ GHz and maximum oscillation frequencies of $f_{max} = 11.5$ GHz have already been demonstrated for emitter dimensions of $4 \times 20 \mu\text{m}^2$.¹ More recently, Chen *et al.*² reported the modulation frequency of 4.5 GHz for the GaAs/AlGaAs ridge waveguide lasers of $10 \times 380 \mu\text{m}^2$ grown on Si substrates. Associated with the growth of GaAs on Si, however, are a number of problems including a 4% lattice mismatch between GaAs and Si. Device performance is limited by the quality of the GaAs layers, which is determined by defects such as misfit dislocations and stacking faults propagating from GaAs/Si interface to the active device area. To minimise the dislocations and suppress their propagation to the surface, a great deal of effort has been made such as *ex situ* annealing^{3,4} and hydrogenation⁵ as well as utilising strained-layer superlattices.⁶ Since the bipolar transistor is very sensitive to any defects such as threading dislocations, it can be used as a

probe to investigate the material properties of GaAs on Si. In addition, *Pnp* GaAs/AlGaAs HBTs on Si have not been studied prior to this work. As a result, we have undertaken an investigation of GaAs/AlGaAs *Pnp* HBTs on Si because of their suitability for many applications such as current sources in I^2L inverters.⁷ In this letter, we report our results on self-aligned GaAs/AlGaAs *Pnp* HBTs grown directly on Si substrates by molecular beam epitaxy for the first time.

The epitaxial structures of GaAs/AlGaAs *Pnp* HBTs reported here were prepared by molecular beam epitaxy (MBE) on Si substrates tilted 4° off (100) toward (110). A $2\mu\text{m}$ GaAs buffer layer doped with Be to $2 \times 10^{18}\text{cm}^{-3}$ was first grown directly on Si substrates, followed by a $0.5\mu\text{m}$ GaAs collector doped with Be to $5 \times 10^{17}\text{cm}^{-3}$, and a 1500\AA GaAs base doped with Si to 10^{19}cm^{-3} . Next, a $0.3\mu\text{m}$ $\text{Al}_{0.3}\text{Ga}_{0.7}\text{As}$ emitter doped with Be to $2 \times 10^{17}\text{cm}^{-3}$ was grown. Finally, a $0.15\mu\text{m}$ emitter cap layer doped with Be to $1 \times 10^{19}\text{cm}^{-3}$ was deposited to facilitate ohmic contacts formation. After growth, HBTs were fabricated using both mesa isolation and self-alignment processes. A 3:1:50 ($\text{NH}_4\text{OH}:\text{H}_2\text{O}_2:\text{H}_2\text{O}$) etching solution was utilised for emitter and self-aligned base mesas and *n*-type and *p*-type contacts were formed by evaporation and subsequent alloying of AuGe/Ni/Au and AuBe, respectively. The details of the fabrication can be found in the literature.⁸

Fig. 1 shows the inverted curve tracer scans of the common emitter output characteristics for typical *Pnp* GaAs/AlGaAs HBTs on Si substrates. Measured common-emitter current gains for devices with an emitter area of $50 \times 50\mu\text{m}^2$ were around 8 at a collector current density of $1 \times 10^4\text{A/cm}^2$. This value compares well with the current gain of $\beta = 12$ for the GaAs/Al_xGa_{1-x}As *Pnp* HBTs with an emitter Al mole fraction of $x = 0.45$ grown on lattice-matched GaAs substrates.⁹ The output characteristics did not show any negative differential resistance (NDR) at a collector current level up to 280 mA,

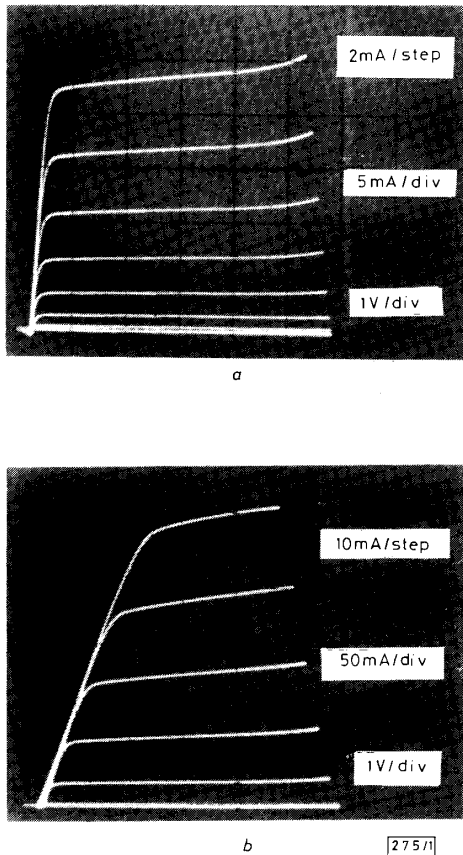


Fig. 1 Inverted photographic pictures of typical common-emitter output characteristics for a *Pnp* HBT with an emitter area of $50 \times 50\mu\text{m}^2$

- a Low current levels
- b High current levels

a phenomenon observed, even at lower current levels by Chand *et al.*¹⁰ for the GaAs/AlGaAs *Pnp* HBTs grown on GaAs substrates. The lack of NDR is tentatively attributed to the better thermal conductivity of Si substrates over GaAs.

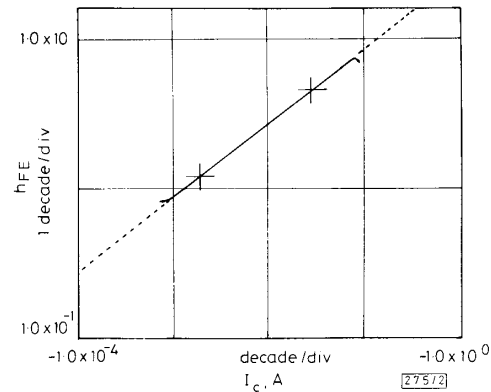


Fig. 2 Logarithmic plot of common-emitter current gain as a function of collector current

The ideality factor of the emitter junction deduced from the slope is approximately 2.0

The measured diode characteristics of emitter-base and base-collector junctions revealed that the turn-on voltages of emitter and collector junctions were 0.7 and 0.8 V, respectively. The base-collector breakdown voltage is as high as 10 V, indicating that threading dislocations, which might penetrate the collector depletion region, do not cause an observable rise in the leakage current. In Fig. 2 is shown the collector current dependence of current gain for *Pnp* transistors on Si. The plotted current gain starts to decrease above a collector current of approximately 100 mA owing to the current limit of HP4145. The ideality factor deduced from the slope of the logarithmic plot is around 2.0, implying the space charge recombination and/or the surface recombination at the exposed periphery of the emitter junction.¹¹ The dependence of measured current gain on the emitter dimensions suggests that the low current gain is in part due to the surface recombination at the emitter junction rather than being entirely an inherent material-related problem of GaAs on Si. Improved current gains can be expected by using the surface passivation or planar structures.^{11,12}

In conclusion, GaAs/AlGaAs *Pnp* HBTs by MBE have been successfully operated on a Si substrate for the first time. A common emitter current gain of $\beta = 8$ was obtained at a collector current density of $1 \times 10^4\text{A/cm}^2$ and the output characteristics did not show any negative differential resistance at a high collector-current level up to 280 mA owing to a better thermal conductivity of Si substrates over GaAs. A very high base-collector breakdown voltage of 10 V was obtained, suggesting that the leakage current is not very sensitive to the dislocations present.

Acknowledgment: This work was funded by the United States Air Force Office of Scientific Research. The CALTECH portion of the research was funded by grants from ONR, AFOSR, ARO and NSF. H. Morkoc was partially funded by SDIO-IST through the Jet Propulsion Laboratory while he was a distinguished visiting scientist.

T. WON
C. W. LITTON*
H. MORKOC

22nd March 1988

Coordinated Science Laboratory
University of Illinois
1101 W. Springfield Avenue
Urbana, IL 61801, USA

A. YARIV
California Institute of Technology
Pasadena, CA 91125, USA

* Permanent address is Avionics Laboratory, Wright Patterson Air Force Base, OH 45433, USA

References

- FISCHER, R., KLEM, J., PENG, C. K., GEDYMIN, J. S., and MORKOC, H.: 'Microwave properties of self-aligned GaAs/AlGaAs hetero-junction bipolar transistors on Si substrates', *IEEE Electron Device Lett.*, 1986, EDL-7, pp. 112-114
- CHEN, H. Z., PASLASKI, J., YARIV, A., and MORKOC, H.: 'High-frequency modulation of AlGaAs/GaAs lasers grown on Si substrates by molecular beam epitaxy', *Appl. Phys. Lett.*, 1988, 52, pp. 605-606
- LEE, J. W., SHICHIJO, H., TSAI, H. L., and MATYI, R. J.: 'Defect reduction by thermal annealing of GaAs layers grown by molecular beam epitaxy on Si substrates', *ibid.*, 1987, 50, pp. 31-33
- CHOI, C., OTSUKA, N., MUNNS, G., HOUDRE, R., MORKOC, H., ZHANG, S. L., LEVI, D., and KLEIN, M. V.: 'Effects of in-situ and ex-situ annealing on dislocations in GaAs on Si substrates', *ibid.*, 1987, 50, pp. 992-994
- PEARTON, S. J., WU, C. S., STAVOLA, M., REN, F., LOPATA, J., DAUTREMONT-SMITH, W. C., VERNON, S. M., and HAVEN, V. E.: 'Hydrogenation of GaAs on Si: effects on reverse leakage current', *ibid.*, 1987, 51, pp. 496-498
- FISCHER, R., MORKOC, H., NEUMANN, D. A., ZABEL, H., CHOI, C., OTSUKA, N., LONGFERBONNE, M., and ERICKSON, L. P.: 'Material properties of high-quality GaAs epitaxial layers grown on Si substrates', *J. Appl. Phys.*, 1986, 60, pp. 1640-1647
- NAROZNY, P., and BENEKING, H.: 'Double heterostructure GaAs/GaAlAs 1^2L inverter', *Electron. Lett.*, 1985, 21, pp. 328-329
- WON, T., PENG, C. K., CHYI, J., and MORKOC, H.: ' $In_{0.52}Al_{0.48}As/In_{0.53}Ga_{0.47}As$ double heterostructure Pnp bipolar transistors by molecular beam epitaxy', submitted to *IEEE Electron Device Lett.*
- FROST, M. S., RICHES, M., and KERR, T.: 'A p-n-p AlGaAs hetero-junction bipolar transistor for high temperature operation', *J. Appl. Phys.*, 1986, 60, pp. 2149-2153
- CHAND, N., HENDERSON, T., FISCHER, R., KOPP, W., and MORKOC, A.: 'A pnp AlGaAs/GaAs heterostructure bipolar transistor', *Appl. Phys. Lett.*, 1985, 46, pp. 302-304
- SANDROFF, C. J., NOTTENBURG, R. N., BISCHOFF, J. C., and BHAT, R.: 'Dramatic enhancement in the gain of a GaAs/AlGaAs hetero-structure bipolar transistor by surface passivation', *ibid.*, 1987, 51, pp. 33-35
- SUNDERLAND, D. A., HADEN, J. M., DZURKO, K. M., STANCHINA, W. E., LEE, H. C., DANNER, A. D., and DAPKUS, P. D.: 'A fully planar p-n-p heterostructure bipolar transistor', *IEEE Electron Device Lett.*, 1988, EDL-9, pp. 116-118

PHOTOCHROMIC BEHAVIOUR OF THULIUM-DOPED SILICA OPTICAL FIBRES

Indexing terms: Photochromism, Optical fibres, Doping, Optical properties of substances

We report the first observation of the photochromic effect in thulium (Tm^{3+}) doped silica optical fibres.

Introduction: There has been a recent increase in interest in optical fibres which exhibit enhanced nonlinear behaviour by virtue of the inclusion of rare-earth ions in the silica host glass.^{1,2} Photochromic behaviour in optical fibres has been observed previously,³ and photorefractive effects have been noted in rare-earth doped silicate and phosphate glasses.⁴ In this letter, we report the first observation of the photochromic effect in thulium (Tm^{3+})-doped silica optical fibres.

Thulium ions were incorporated in the GeO_2/P_2O_5 core region of a silica fibre in a concentration of several hundred parts per million. The solution deposition method was used,⁵ which is a variant of the MCVD process of fibre manufacture. The core radius was about $3\mu m$ and the V -value at 500 nm wavelength was approximately 5. In the 'as drawn' state, the thulium ions in the glass matrix exhibit an absorption spectrum shown in Fig. 1. The important features of this spectrum are the absorption band $^3H_6 \rightarrow ^1G_4$ ⁶ between wavelengths of 450 nm and 485 nm, and the relatively high transmissivity between 485 nm and 650 nm. When the fibre was illuminated with light at a wavelength of 475 nm from a CW argon-ion laser, the transmission of this wavelength was found to decrease with time, that is to exhibit photodarkening or

colouration. After several minutes exposure to 100 mW launched optical power at 475 nm wavelength, the attenuation of the pump increased from 20 dB to 30 dB in a 4 m length of fibre. This darkening process was apparent only when pumping into the $^3H_6 \rightarrow ^1G_4$ absorption band. The magnitude of the timescales indicated that the effect was attributable to structural changes in the glass in the vicinity of the thulium ions.

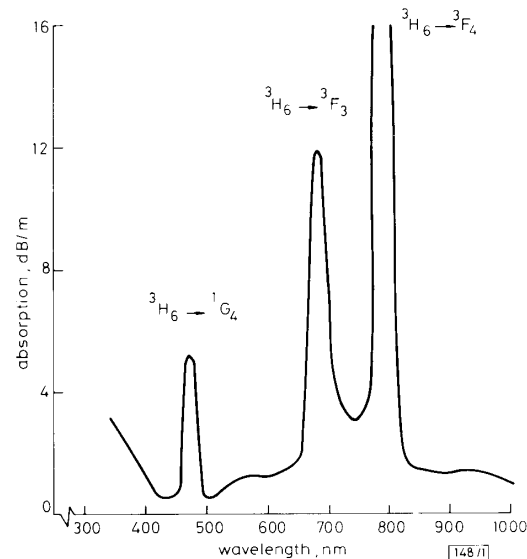


Fig. 1 Absorption spectrum of 'as drawn' thulium-doped silica fibre

Experiments: In the visible to near-IR region of the spectrum, we measured the change in optical transmission through a length of thulium-doped fibre between the transparent (state I) and coloured (state II) conditions, induced by pumping at 475 nm wavelength. Probe wavelengths were 475 nm, 514 nm, 633 nm and filtered white light between 600 nm and 1000 nm. Fig. 2 shows the maximum change in transmission with induced colouration. The pump power was 300 mW and the exposure time was 5 min, conditions which saturated the induced absorption. The broad absorption band created by the colour-centre formation extends in wavelength from less than 500 nm to greater than 800 nm. The ground-state absorptions of the thulium ions around 690 nm and 800 nm precluded accurate measurement of the induced absorption in these regions. The broken curve in Fig. 2 joins discrete data points.

It was found that the darkening could be reversed by pumping the fibre at a wavelength of 514 nm. The fibre reverted to its 'as drawn' condition (state I) within similar timescales and for similar optical powers required to create the colour centres. It is thought that the reversing process is due to thermal relaxation.

The exposure conditions were studied in greater detail, using a 60 cm length of fibre doped with 1000 parts per million of thulium ions. It should be noted that this fibre was drawn from a different preform from the fibre discussed previously, indicating that the effect was not restricted to one

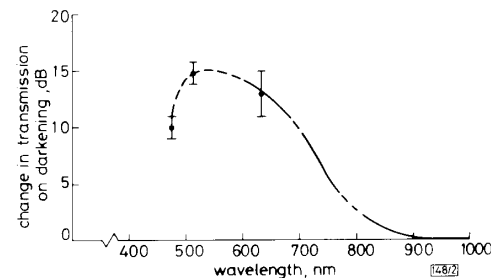


Fig. 2 Change in transmission through a 4 m length of thulium-doped silica fibre after illumination at 475 nm wavelength